

## Polymers critical point originates Brownian non-Gaussian diffusion

Sankaran Nampoothiri,<sup>\*</sup> Enzo Orlandini,<sup>†</sup> Flavio Seno,<sup>‡</sup> and Fulvio Baldovin<sup>§</sup>

*Dipartimento di Fisica e Astronomia “G. Galilei”–DFA, Sezione INFN, Università di Padova, Via Marzolo 8, 35131 Padova (PD), Italy*



(Received 8 October 2021; accepted 11 December 2021; published 30 December 2021)

We demonstrate that size fluctuations close to polymers critical point originate the non-Gaussian diffusion of their center of mass. Static universal exponents  $\gamma$  and  $\nu$ —depending on the polymer topology, on the dimension of the embedding space, and on equilibrium phase—concur to determine the potential divergency of a dynamic response, epitomized by the center-of-mass kurtosis. Prospects in experiments and stochastic modeling brought about by this result are briefly outlined.

DOI: [10.1103/PhysRevE.104.L062501](https://doi.org/10.1103/PhysRevE.104.L062501)

As a consequence of the central limit theorem, ordinary diffusive motion of mesoscopic particles in solution is characterized by a Gaussian probability density function (PDF) whose variance grows linearly over time. Numerous experiments performed in complex contexts [1–16], while confirming the linear temporal increase of the variance, highlight, however, distinct stages during which the PDF of the random motion is non-Gaussian. This interesting contingency has been called “Brownian non-Gaussian diffusion” and has inspired various mesoscopic approaches, invoking superposition of statistics [2,15,17,18], diffusing diffusivities [19–26], subordination concepts [20], continuous-time random walk [27], and diffusion in disordered environments [28], but presently few attempts have been made to establish a microscopic foundation of this phenomenon [29,30]. To breach the central limit theorem [31] one possibility is the emergence of strong correlations; here we demonstrate that the polymers critical point, separating the dilute to the dense phase in the grand canonical ensemble [32–35], indeed originates a Brownian yet non-Gaussian diffusion for the center of mass (c.m.) of a polymer in solution. Prospects in experiments and stochastic modeling brought about by this result are briefly outlined.

Consider the grand canonical description of an isolated polymer in solution in contact with a monomer chemostat. The size of the polymer  $N$  is a random variable and to the event  $N = n \in \mathbb{N}$  is associated an equilibrium distribution  $P_N^*(n)$  determined by the monomer fugacity  $z$ . Close to criticality  $z \rightarrow z_c^-$  the partition function asymptotically behaves as

$$Z_{\text{gc}}(z) = \sum_n (\mu_c z)^n n^{\gamma-1} \sim \begin{cases} (1 - z/z_c)^{-\gamma} & (\gamma > 0) \\ -\ln(1 - z/z_c) & (\gamma = 0) \\ \text{finite} & (\gamma < 0), \end{cases} \quad (1)$$

where  $\mu_c$  is the (model-dependent) connective constant and  $z_c = \mu_c^{-1}$ . The entropic exponent  $\gamma$  is specified by the space dimension  $d$  and by the topology of the polymeric structure (homeomorphism type of the underlying graph); together with the metric exponent  $\nu > 0$  it identifies the universality class of the critical behavior. For the wide class of polymer networks in good solvent conditions, with any prescribed fixed topology  $\mathcal{G}$  made of chains of equal lengths, this exponent is known thanks to the mapping with the magnetic  $O(n \rightarrow 0)$  model [33] through the relation [36]

$$\gamma = \gamma_{\mathcal{G}} = 1 - \nu d \mathcal{L} + \sum_{L \geq 1} n_L \sigma_L, \quad (2)$$

where  $\mathcal{L}$  is the number of physical loops (or cyclomatic number) in the polymer network,  $n_L$  the number of vertices with functionality  $L$ , and  $\sigma_L$  the associated scaling dimension (see Fig. 1 for examples and further details). Also in the case when monomers functionality is free to fluctuate as in lattice animals and trees [34,37], the  $\gamma$  exponent can be exactly computed by relating the critical behavior of these systems to the Yang-Lee singularity of an Ising model in  $d - 2$  dimensions [38,39] (again, more details in Fig. 1). The metric exponent characterizes the large  $N$  behavior of the average square end-to-end distance of large polymer chains:  $R^2 \sim N^{2\nu}$ . Unlike the entropic one, its value does not depend on topology (if fixed) but on the dimension of the embedding space (see Fig. 1). Note that both exponents can further depend on the polymer being in different equilibrium phases such as those triggered by monomer-monomer attractions (coil to globule transition) or by effective interactions with impenetrable surfaces (adsorption transition) [32,34].

The position of the polymer c.m.  $\mathbf{R}_{\text{c.m.}}(t) = (X_{\text{c.m.}}(t), Y_{\text{c.m.}}(t), Z_{\text{c.m.}}(t))$  undergoes a Brownian motion described by [45]

$$d\mathbf{R}_{\text{c.m.}}(t) = \sqrt{2D(N(t))} d\mathbf{B}(dt), \quad (3)$$

where  $\mathbf{B}(t)$  is a Wiener process (Brownian motion). In view of the Stokes-Einstein relation [46–48]

$$D(N) \sim D_0/N^\nu, \quad (4)$$

<sup>\*</sup>sankaran.nampoothiri@unipd.it

<sup>†</sup>orlandini@pd.infn.it

<sup>‡</sup>flavio.seno@unipd.it

<sup>§</sup>fulvio.baldovin@unipd.it

Polymer topology	$d = 2$		$d = 3$	
	$\nu_G$	$\Upsilon_G$	$\nu_G$	$\Upsilon_G$
	$\frac{3}{4}$	$\frac{43}{32}$	0.5882 (11) 0.587 597 (7)	$\cong \frac{9}{8}; 1.15695300(95)$
	$\frac{3}{4}$	$1 + \mathcal{R} \frac{11}{64} + \frac{(2 - \mathcal{R})(9\mathcal{R} + 2)}{64}$	0.5882 (11) 0.587 597 (7)	$1 + \frac{\mathcal{R}}{16} + (2 - \mathcal{R}) \frac{\mathcal{R}}{16}$
	$\frac{3}{4}$	$1 - \nu d = -\frac{1}{2}$	0.5882 (11) 0.587 597 (7)	$1 - \nu d = -0.761$
	$\frac{3}{4}$	$1 - \nu d \mathcal{L} + 2\sigma_{\mathcal{L}+1}$	0.5882 (11) 0.587 597 (7)	$1 - \nu d \mathcal{L} + 2\sigma_{\mathcal{L}+1}$
	0.64115 (5)	$\theta = 1$ $\gamma = 1 - \theta = 0$	$\frac{1}{2}$	$\theta = \frac{3}{2}$ $\gamma = 1 - \theta = -\frac{1}{2}$

FIG. 1. Metric and entropic exponents of different polymer network topologies (i.e., homeomorphism types) in  $d = 2$  and  $d = 3$  under good solvent conditions. The first row refers to linear self-avoiding polymers: values in  $d = 2$  are exact and were first computed via Coulomb gas [40];  $d = 3$  values have been originally obtained by Wilson-Fisher expansion in dimension  $d = \epsilon - 4$  for the  $\varphi^4$  field theory of the  $O(n \rightarrow 0)$  model with  $\epsilon = 1$  [41] (first number), and later estimated with high precision Monte Carlo simulations [42,43] (second number). Exponents from the second to the fourth row refer to star polymers with  $\mathcal{R}$  arms [36], ring polymers, and watermelon graphs with  $\mathcal{L}$  independent loops [36], respectively. Since topology is kept fixed, the  $\nu$  exponent does not vary with respect to the linear case. The  $\gamma$  exponent is obtained filling proper values for  $\nu, d, \mathcal{L}, n_L$  in Eq. (2), together with  $\sigma_L = (2 - L)(9L + 2)/64$  (exact,  $d = 2$ ) or  $\sigma_L = \epsilon(2 - L)L/16 + O(\epsilon^2)$  ( $d = 3$ ). For instance, with star polymers one has  $\mathcal{L} = 0, n_1 = \mathcal{R}$ , and  $n_{\mathcal{R}} = 1$  (the  $n_2$  monomers with functionality  $L = 2$  do not contribute as  $\sigma_2 = 0$ ); note that the two-arms topology ( $n_1 = 2, \mathcal{R} = 2$ ) corresponds to linear polymer. Similarly, with watermelon graphs  $\mathcal{L} \geq 1, n_{\mathcal{L}+1} = 2$ . The last row refers instead to lattice animals, i.e., polymers in which the number of loops and branches can vary. In this case critical exponents in  $d$  dimensions are related to the Lee-Yang edge singularity [38] through the relations  $\nu_{d+2} = (\beta_d + 1)/2$  and  $\theta_{d+2} = \beta_d + 2$ , where  $\beta_d$  is the exponent controlling magnetization near the edge singularity. As the latter is exactly solvable in  $d = 0$  and  $d = 1$  with  $\beta_0 = -1$  and  $\beta_1 = -1/2$ , respectively, one gets  $\gamma_2 = 1 - \theta_2 = 0, \gamma_3 = 1 - \theta_3 = -1/2$ , and  $\nu_3 = 3/2$ . The exact expression for  $\nu_{d+2}$ , however, breaks down with  $d = 0$  and for  $\nu_2$  one has to rely on numerical estimates [44], such as the one reported in the table. Note that with  $d \geq 3$  exponents  $\gamma$  and  $\nu$  are not independent but follow the relation  $\gamma = 1 - (d - 2)\nu$ .

with  $D_0$  specific to the polymer subunits. Under the present assumptions  $D$  fluctuates with the polymer size: we see that  $\mathbf{R}_{\text{c.m.}}(t)$  becomes thus a subordinated stochastic process [31] conditioned by the history  $[n(t)] \equiv \{n(t') \in \mathbb{N} | 0 \leq t' \leq t\}$  of the polymer size. It is convenient to reparametrize the diffusion path in terms of the coordinate  $s \geq 0, ds = 2D(n(t))dt$ , corresponding to the realization of the stochastic process

$$S(t) \equiv 2 \int_0^t dt' D(N(t')) = 2D_0 \int_0^t dt' N^{-\nu}(t'). \quad (5)$$

By using the subordination formula [31,50]

$$p_{\mathbf{R}_{\text{c.m.}}}(\mathbf{r}, t | n_0; \mathbf{0}) = \int_0^\infty ds \frac{e^{-r^2/2s}}{(2\pi s)^{3/2}} p_S(s, t | n_0), \quad (6)$$

where  $p_{\mathbf{R}_{\text{c.m.}}}(\mathbf{r}, t | n_0; \mathbf{0})$  is the c.m. conditional PDF given the initial condition  $p_{\mathbf{R}_{\text{c.m.}}}(\mathbf{r}, 0 | n_0; \mathbf{0}) = \delta_{n, n_0} \delta(\mathbf{r})$ , moments of the subordinated process are straightforwardly connected to those of the subordinator. For instance, assuming an equilibrium distribution  $P_N^*(n_0)$  for the initial size,

$$\mathbb{E}[X_{\text{c.m.}}^2(t)] = \mathbb{E}[S(t)], \quad \mathbb{E}[X_{\text{c.m.}}^4(t)] = 3 \mathbb{E}[S^2(t)]. \quad (7)$$

We already appreciate the influence of  $\gamma$  and  $\nu$  in these moments: while the latter enters in the definition of  $S(t)$ , the former characterizes  $P_N^*(n)$ .

Importantly, the equilibrium distribution  $P_N^*(n)$  can be related to a simple master equation describing the polymerization/depolymerization process occurring as monomers add and detach to the polymer in the grand canonical ensemble. First of all we observe that if  $n_{\min}$  is the minimal polymer size, through the change of variable  $n \mapsto n - (n_{\min} - 1)$  we can always associate the support  $1 \leq n < \infty$  to  $P_N^*(n)$  without altering the asymptotic behavior in Eq. (4). Regard then the (forward) master equation

$$\begin{aligned} \partial_t P_N(n, t | n_0) &= \mu P_N(n + 1, t | n_0) \quad (n > 1) \\ &\quad + \lambda(n - 1) P_N(n - 1, t | n_0) \\ &\quad - [\mu + \lambda(n)] P_N(n, t | n_0), \\ \partial_t P_N(1, t | n_0) &= \mu P_N(2, t | n_0) - \lambda(1) P_N(1, t | n_0). \end{aligned} \quad (8)$$

Here  $P_N(n, t | n_0)$  is the probability for  $N = n$  at time  $t \geq 0$  given  $N = n_0$  at  $t = 0$ , and  $\lambda(n), \mu$  are the rates for association and dissociation, respectively. Defining the growth factor as  $g(n) \equiv \lambda(n)/\mu$ , it is straightforward to prove that

stationarity is attained under detailed balance,  $g(n) = P_N^*(n+1)/P_N^*(n) = \mu_c z [(n+1)/n]^{\gamma-1}$ : this identifies the polymerization process, given  $P_N^*(n)$ . In *chain polymerization* [51], while it is natural to consider dissociation to be independent of the polymer size, aggregation is instead influenced by the ratio of the number of available configurations at sizes  $n+1$  and  $n$ . This is the reason for the size dependency  $\lambda(n)$  assumed here, which is conveyed by the entropic correction  $\propto n^{\gamma-1}$  outside the mean-field limit ( $\gamma \neq 1$ ). Note that the rate  $\mu$  remains a free parameter which may rescale Eq. (8), thus determining the timescale  $\tau$  for the autocorrelation of  $N(t)$ . This is particularly apparent in the mean-field case ( $\gamma = 1$ ), where an elegant connection with the  $M/M/1$  model (Markovian interarrival times/Markovian service times/one server) in queuing theory [52] allows one to extend the identification even outside criticality and to analytically solve both the equilibrium and the out-of-equilibrium behavior [53]. The asymptotic behavior for small and large time of  $P_N(n, t|n_0)$  is  $P_N(n, t|n_0)_{t \ll \tau} \sim \delta_{n, n_0}$ ,  $P_N(n, t|n_0)_{t \gg \tau} \sim P_N^*(n)$ , respectively.

The equilibrium size distribution is directly deduced from the grand canonical partition function (generating function). Close to the critical point  $z_c = 1/\mu_c$  we may neglect regular contributions, and, remembering the definition of polylogarithm functions,  $\text{Li}_s(z) \equiv \sum_{n=1}^{\infty} z^n/n^s$  (which are finite in  $z = 1$  if  $s > 1$ ), we have

$$P_N^*(n) = \frac{(z/z_c)^n}{n^{1-\gamma} \text{Li}_{1-\gamma}(z/z_c)} \sim \begin{cases} \frac{(1-z/z_c)^\gamma (z/z_c)^n}{n^{1-\gamma} \Gamma(\gamma)} & (\gamma > 0) \\ -\frac{(z/z_c)^n}{n \ln(1-z/z_c)} & (\gamma = 0) \\ \frac{(z/z_c)^n}{n^{1-\gamma} \text{Li}_{1-\gamma}(z/z_c)} & (\gamma < 0). \end{cases} \quad (9)$$

We are now in a position to evaluate expected values in Eq. (7). Let us primarily note that, with equilibrium initial conditions  $P_N^*(n_0)$ ,

$$\begin{aligned} \mathbb{E}[S(t)] &\sim 2D_0 \int_0^t dt' \sum_{n, n_0} \frac{P_N(n, t'|n_0) P_N^*(n_0)}{n^\nu} \\ &= 2D_0 t \mathbb{E}[N^{-\nu}], \end{aligned} \quad (10)$$

where we have used the stationarity of  $P_N^*(n)$ . Together with Eq. (7), this proves the Brownian character of the c.m. diffusion in equilibrium. Transients may display either sub- or superdiffusive stages, depending on the specific initial condition [53]. Using the asymptotic expressions for  $P_N(n, t|n_0)$ , we analogously find

$$\mathbb{E}[S^2(t)] \sim \begin{cases} (2D_0 t)^2 \mathbb{E}[N^{-2\nu}] & (t \ll \tau) \\ (2D_0 t)^2 (\mathbb{E}[N^{-\nu}])^2 & (t \gg \tau), \end{cases} \quad (11)$$

which implies, for the c.m. kurtosis,

$$\kappa_{\text{c.m.}}(t) = \frac{3 \mathbb{E}[S^2(t)]}{(\mathbb{E}[S(t)])^2} \sim \begin{cases} 3 \frac{\mathbb{E}[N^{-2\nu}]}{(\mathbb{E}[N^{-\nu}])^2} & (t \ll \tau) \\ 3 \text{ (Gaussian)} & (t \gg \tau). \end{cases} \quad (12)$$

Equation (12) shows that, while the kurtosis is potentially different from 3 for time within the scale  $\tau$ , it crosses over to the Gaussian value at larger time. This is specifically what is observed in many experiments [1,2,7,12–14] and also obtained in various mesoscopic models [20–22,24,26,54].

TABLE I. Behavior of the initial c.m. kurtosis.

$\gamma > 0$	
$\nu$	$\kappa_{\text{c.m.}}(t)_{t \ll \tau} \sim$
$0 < \nu < \gamma/2$	$3 \frac{\Gamma(\gamma) \Gamma(\gamma-2\nu)}{[\Gamma(\gamma-\nu)]^2} \text{ (finite)}$
$0 < \nu = \gamma/2$	$3 \frac{\Gamma(\gamma)}{[\Gamma(\gamma/2)]^2} [-\ln(1-z/z_c)]$
$\gamma/2 < \nu < \gamma$	$3 \frac{\Gamma(\gamma) \text{Li}_{1-\gamma+2\nu}(z/z_c)}{[\Gamma(\gamma-\nu)]^2} \frac{1}{(1-z/z_c)^{2\nu-\gamma}}$
$\nu = \gamma$	$3 \frac{\Gamma(\gamma) \text{Li}_{\gamma+1}(z/z_c)}{(1-z/z_c)^\gamma [-\ln(1-z/z_c)]^2}$
$\nu > \gamma$	$3 \frac{\Gamma(\gamma) \text{Li}_{1-\gamma+2\nu}(z/z_c)}{[\text{Li}_{1-\gamma+\nu}(z/z_c)]^2} \frac{1}{(1-z/z_c)^\gamma}$
$\gamma = 0$	
$\nu > 0$	$3 \frac{\text{Li}_{1+2\nu}(z/z_c)}{[\text{Li}_{1+\nu}(z/z_c)]^2} [-\ln(1-z/z_c)]$
$\gamma < 0$	
$\nu > 0$	$3 Z_{\text{gc}}(z) \frac{\text{Li}_{1-\gamma+2\nu}(z/z_c)}{[\text{Li}_{1-\gamma+\nu}(z/z_c)]^2} \text{ (finite)}$

To evaluate the non-Gaussianity of the c.m. diffusion in terms of  $\kappa_{\text{c.m.}}$  during the early stages, averages in Eq. (12) must be calculated according to Eq. (9). Once more, this invokes the known behavior of the polylogarithm function; it also highlights the interplay between exponents  $\gamma, \nu$  in establishing the dynamic response. We have

$$\kappa_{\text{c.m.}}(t)_{t \ll \tau} \sim \frac{3}{\text{Li}_{1-\gamma}(z/z_c)} \frac{\text{Li}_{1-\gamma+2\nu}(z/z_c)}{[\text{Li}_{1-\gamma+\mu}(z/z_c)]^2}. \quad (13)$$

Table I wraps up the initial kurtosis behavior, which includes power-law divergency (possibly with logarithmic corrections), logarithmic divergency, or even finiteness. The shape of the initial non-Gaussian PDF for the polymer c.m. is conveniently studied by switching to the unit-variance dimensionless variable  $\bar{X}_{\text{c.m.}}(t) \equiv X_{\text{c.m.}}(t)/\sqrt{\mathbb{E}[X^2(t)]}$ . From

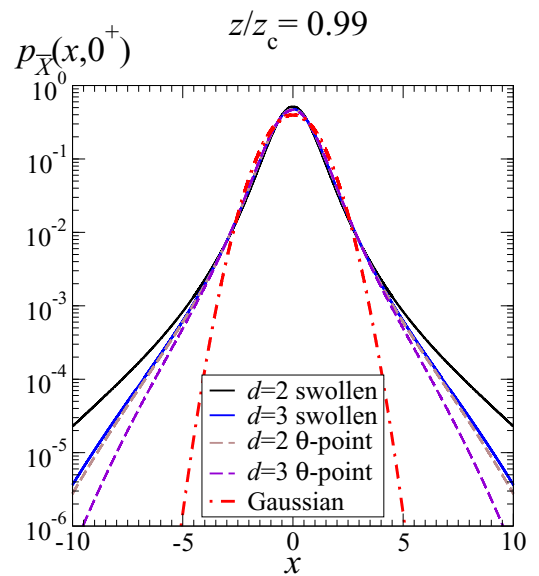


FIG. 2. Unit-variance initial  $x$  PDF for the c.m. of a linear polymer close to criticality. For comparison purposes, a unit-variance Gaussian PDF is also plotted in a red dash-dotted line.

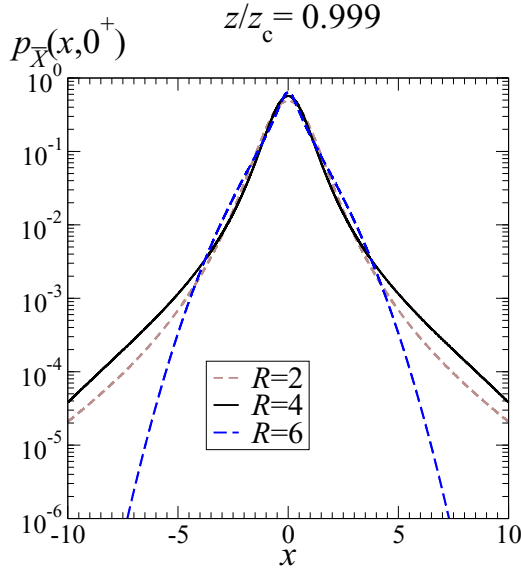


FIG. 3. Unit-variance initial  $x$  PDF for the c.m. of a star polymer in  $d = 3$  with different numbers of arms  $\mathcal{R}$  close to criticality.

Eq. (6), as  $t \rightarrow 0^+$ , we have

$$p_{\bar{X}}(x, 0^+) \sim \sum_{n=1}^{\infty} P_N^*(n) \frac{e^{-\mathbb{E}[N^{-\nu}]x^2/2n^{-\nu}}}{\sqrt{2\pi \frac{n^{-\nu}}{\mathbb{E}[N^{-\nu}]}}}, \quad (14)$$

which only depends on  $z/z_c$ ,  $\gamma$ , and  $\nu$ . At large  $|x|$  the PDF is asymptotic to the Gaussian cutoff  $\sim e^{-\mathbb{E}[N^{-\nu}]x^2/2}$ , and as  $z/z_c \rightarrow 1$  this cutoff is pushed towards  $|x| \rightarrow \infty$ , since  $\mathbb{E}[N^{-\nu}] \rightarrow 0$ .

It is now interesting to discuss peculiar initial dynamical responses of polymers with different topologies, as  $z \rightarrow z_c$ .

*Linear polymers.* In this case the condition  $\gamma/2 < \nu < \gamma$  is satisfied both in  $d = 2$  and  $d = 3$  (see first row in Fig. 1) and the kurtosis diverges with exponents  $5/32$  and  $\simeq 0.012$ , respectively (cf. Fig. 2).

*$\mathcal{R}$ -arms star polymers.* In  $d = 2$  the kurtosis diverges if  $\mathcal{R} \leq 4$ , with exponent  $2\nu - \gamma$  ( $\mathcal{R} = 2, 3$ ) or  $\gamma$  ( $\mathcal{R} = 4$ ). In  $d = 3$  the kurtosis diverges if  $\mathcal{R} \leq 5$ , with exponent  $2\nu - \gamma$  ( $\mathcal{R} = 2, 3, 4$ ) or  $\gamma$  ( $\mathcal{R} = 5$ ) (cf. Fig. 3).

*Rings and watermelon networks.* Since  $\gamma < 0$  both in  $d = 2$  and  $d = 3$ ,  $\kappa_{c.m.}$  does not diverge.

*Branched polymers (lattice animals).* In  $d = 2$ ,  $\gamma = 0$  and the kurtosis diverges logarithmically, independently on the value of  $\nu$ . Instead, in  $d = 3$ ,  $\gamma < 0$ , implying a finite value of  $\kappa_{c.m.}$  also at the critical point.

So far we have considered polymers whose equilibrium properties are dominated by monomer-solvent attraction (swollen phase). On the other hand, by varying solvent

conditions polymers may undergo a thermodynamic transition from swollen (good solvent) to globular or compact phase (poor solvent). The transition occurs at a well-defined critical phase known as  $\Theta$  point, a genuine  $O(n \rightarrow 0)$  tricritical point governing an equilibrium phase characterized by its own critical exponents  $\gamma_{\Theta}$  and  $\nu_{\Theta}$  [32,34]. For instance, linear polymers at the  $\Theta$  point in  $d = 2$  have  $\nu_{\Theta} = 4/7$  and  $\gamma_{\Theta} = 8/7$  [55–58], whereas in  $d = 3$  the mean-field values  $\nu_{\Theta} = 1/2$  and  $\gamma_{\Theta} = 1$  are expected [33,59]. Hence, in both dimensions  $\nu = \gamma/2$ . This remarkable relation has the important consequence that as  $z \rightarrow z_c$  the initial kurtosis diverges logarithmically for linear polymers at the  $\Theta$  point, irrespective of the dimension. This result suggests that a change in the quality of the solvent driving dilute linear polymers close to  $\Theta$  point, concomitantly mitigates the non-Gaussianity of the c.m. diffusion from power-law to logarithmic divergence of  $\kappa_{c.m.}$ . Figure 2 displays the associated PDFs.

Finally, since the  $\nu$  and  $\gamma$  exponents depend on the embedding dimension  $d$  of the system, transitions between phases with different effective dimension may also alter the non-Gaussianity of the initial c.m. diffusion. An example is the well-studied [32,34] adsorption transition from the  $d = 3$  polymer swollen phase to the adsorbed ( $d = 2$ ) swollen phase. This is triggered by effective attractive interactions between monomers and an impenetrable surface. With a non-negligible mobility of the polymer at the surface, the adsorption transition of linear polymers increases the exponent of the power-law divergence of  $\kappa_{c.m.}$  from 0.012 ( $d = 3$ ) to  $5/32$  ( $d = 2$ ).

We have analytically shown that the polymer critical state is the hallmark behind the non-Gaussian behavior of its c.m. To each universality class, identified by the entropic and metric exponents  $\gamma$  and  $\nu$ , corresponds a specific Brownian non-Gaussian diffusion of the polymer c.m. which crosses then over to ordinary Brownian motion above the polymerization autocorrelation timescale. This finding offers novel perspectives in stochastic modeling, as the anomalous stochastic process is not obtained here via a mesoscopic ansatz, but rather as a natural consequence of a microscopic foundation which can be worked out in all details and bridges the universal behavior of polymer systems at equilibrium with their short-time anomalous dynamical response. The background we have evoked (different polymer architectures,  $\Theta$ , and adsorption transitions) is commonly operated in polymer experiments; this implies the exposed anomalous dynamics to be potentially triggered and highlighted in a variety of chemostatted experimental conditions.

We acknowledge insightful discussions with R. Metzler. This work has been partially supported by the University of Padova BIRD191017 project “Topological statistical dynamics.”

- [1] B. Wang, S. M. Anthony, S. C. Bae, and S. Granick, *Proc. Natl. Acad. Sci. U.S.A.* **106**, 15160 (2009).  
 [2] B. Wang, J. Kuo, S. C. Bae, and S. Granick, *Nat. Mater.* **11**, 481 (2012).

- [3] T. Toyota, D. A. Head, C. F. Schmidt, and D. Mizuno, *Soft Matter* **7**, 3234 (2011).  
 [4] I. Chakraborty and Y. Roichman, *Phys. Rev. Res.* **2**, 022020(R) (2020).

- [5] E. R. Weeks, J. C. Crocker, A. C. Levitt, A. Schofield, and D. A. Weitz, *Science* **287**, 627 (2000).
- [6] C. E. Wagner, B. S. Turner, M. Rubinstein, G. H. McKinley, and K. Ribbeck, *Biomacromolecules* **18**, 3654 (2017).
- [7] J.-H. Jeon, M. Javanainen, H. Martinez-Seara, R. Metzler, and I. Vattulainen, *Phys. Rev. X* **6**, 021006 (2016).
- [8] E. Yamamoto, T. Akimoto, A. C. Kalli, K. Yasuoka, and M. S. Sansom, *Sci. Adv.* **3**, e1601871 (2017).
- [9] S. Stylianidou, N. J. Kuwada, and P. A. Wiggins, *Biophys. J.* **107**, 2684 (2014).
- [10] B. R. Parry, I. V. Surovtsev, M. T. Cabeen, C. S. O'Hern, E. R. Dufresne, and C. Jacobs-Wagner, *Cell* **156**, 183 (2014).
- [11] M. C. Munder, D. Midtvedt, T. Franzmann, E. Nuske, O. Otto, M. Herbig, E. Ulbricht, P. Müller, A. Taubenberger, S. Maharana *et al.*, *eLife* **5**, e09347 (2016).
- [12] A. G. Cherstvy, O. Nagel, C. Beta, and R. Metzler, *Phys. Chem. Chem. Phys.* **20**, 23034 (2018).
- [13] Y. Li, F. Marchesoni, D. Debnath, and P. K. Ghosh, *Phys. Rev. Res.* **1**, 033003 (2019).
- [14] A. Cuetos, N. Morillo, and A. Patti, *Phys. Rev. E* **98**, 042129 (2018).
- [15] S. Hapca, J. W. Crawford, and I. M. Young, *J. R. Soc., Interface* **6**, 111 (2008).
- [16] R. Pastore, A. Ciarlo, G. Pesce, F. Greco, and A. Sasso, *Phys. Rev. Lett.* **126**, 158003 (2021).
- [17] C. Beck and E. G. Cohen, *Physica A* **322**, 267 (2003).
- [18] C. Beck, *Prog. Theor. Phys. Suppl.* **162**, 29 (2006).
- [19] M. V. Chubynsky and G. W. Slater, *Phys. Rev. Lett.* **113**, 098302 (2014).
- [20] A. V. Chechkin, F. Seno, R. Metzler, and I. M. Sokolov, *Phys. Rev. X* **7**, 021002 (2017).
- [21] R. Jain and K. Sebastian, *J. Chem. Sci.* **129**, 929 (2017).
- [22] N. Tyagi and B. J. Cherayil, *J. Phys. Chem. B* **121**, 7204 (2017).
- [23] T. Miyaguchi, *Phys. Rev. E* **96**, 042501 (2017).
- [24] V. Sposini, A. V. Chechkin, F. Seno, G. Pagnini, and R. Metzler, *New J. Phys.* **20**, 043044 (2018).
- [25] V. Sposini, A. Chechkin, and R. Metzler, *J. Phys. A: Math. Theor.* **52**, 04LT01 (2018).
- [26] J. M. Miotto, S. Pigolotti, A. V. Chechkin, and S. Roldán-Vargas, *Phys. Rev. X* **11**, 031002 (2021).
- [27] E. Barkai and S. Burov, *Phys. Rev. Lett.* **124**, 060603 (2020).
- [28] A. Pacheco-Pozo and I. M. Sokolov, *Phys. Rev. Lett.* **127**, 120601 (2021).
- [29] F. Baldovin, E. Orlandini, and F. Seno, *Front. Phys.* **7**, 124 (2019).
- [30] M. Hidalgo-Soria and E. Barkai, *Phys. Rev. E* **102**, 012109 (2020).
- [31] W. Feller, *An Introduction to Probability Theory and Its Applications* (Wiley, New York, 1968).
- [32] P.-G. de Gennes, *Phys. Lett. A* **38**, 339 (1972).
- [33] P.-G. de Gennes, *Scaling Concepts in Polymer Physics* (Cornell University Press, Ithaca, 1979).
- [34] C. Vanderzande, *Lattice Models of Polymers* (Cambridge University Press, Cambridge, UK, 1998).
- [35] N. Madras and G. Slade, *The Self-Avoiding Walk* (Springer, New York, 2013).
- [36] B. Duplantier, *J. Stat. Phys.* **54**, 581 (1989).
- [37] T. C. Lubensky and J. Isaacson, *Phys. Rev. A* **20**, 2130 (1979).
- [38] G. Parisi and N. Sourlas, *Phys. Rev. Lett.* **46**, 871 (1981).
- [39] D. C. Brydges and J. Z. Imbrie, *Ann. Math.* **158**, 1019 (2003).
- [40] B. Nienhuis, *Phys. Rev. Lett.* **49**, 1062 (1982).
- [41] R. Guida and J. Zinn-Justin, *J. Phys. A* **31**, 8103 (1998).
- [42] N. Clisby, *Phys. Rev. Lett.* **104**, 055702 (2010).
- [43] N. Clisby, *J. Phys. A: Math. Theor.* **50**, 264003 (2017).
- [44] I. Jensen, *J. Stat. Phys.* **102**, 865 (2001).
- [45] This equation applies to the Smoluchowski timescale; the latter is appropriate for the description of the polymer dynamics at any sizes  $N$  varying from single monomer to large colloids. Indeed, in the time needed to lose memory of inertial effects, the traveled distance with respect to the polymer radius  $a$  is given by  $\sqrt{3mk_B T}/(6\pi\eta a^2)$ . In water at room temperature, this ratio varies from  $10^{-3}$  for single nucleotides or amino acids to  $10^{-5}$  for large colloids.
- [46] M. Doi and S. F. Edwards, *The Theory of Polymer Dynamics* (Oxford University Press, New York, 1992).
- [47] E. Yamamoto, T. Akimoto, A. Mitsutake, and R. Metzler, *Phys. Rev. Lett.* **126**, 128101 (2021).
- [48] The value for the diffusion coefficient  $D$  to be filled in Eq. (3) is the one coming from the hydrodynamic radius of the polymer  $R$  [49]. Close to criticality, the latter is determined by the metric exponent  $\nu$  as  $R \sim N^\nu$ . So, Eq. (3) can be considered with both the exact values for the exponent  $\nu$  and their approximations, like, e.g., the Flory one [46,49].
- [49] M. Rubinstein and R. H. Colby, *Polymer Physics* (Oxford University Press, New York, 2003).
- [50] S. Bochner, *Harmonic Analysis and the Theory of Probability* (University of California Press, Berkeley, 2020).
- [51] G. Odian, *Principles of Polymerization* (Wiley, New York, 2004).
- [52] J. L. Jain, S. G. Mohanty, and W. Böhm, *A Course on Queueing Models* (Chapman and Hall, London/CRC, Boca Raton, FL, 2007).
- [53] S. Nampoothiri, E. Orlandini, F. Seno, and F. Baldovin (unpublished).
- [54] W. Wang, F. Seno, I. M. Sokolov, A. V. Chechkin, and R. Metzler, *New J. Phys.* **22**, 083041 (2020).
- [55] B. Duplantier and H. Saleur, *Phys. Rev. Lett.* **59**, 539 (1987).
- [56] B. Duplantier, *Europhys. Lett.* **7**, 677 (1988).
- [57] F. Seno and A. Stella, *J. Phys.* **49**, 739 (1988).
- [58] C. Vanderzande, A. L. Stella, and F. Seno, *Phys. Rev. Lett.* **67**, 2757 (1991).
- [59] B. Duplantier, *J. Phys.* **43**, 991 (1982).